Journal of Environmental Sciences 159 (2026) 250–262

Contents lists available at ScienceDirect

Journal of Environmental Sciences

journal homepage: www.elsevier.com/locate/jes

JES JOURNAL OF ENVIRONMENTAL SCIENCES www.jesc.ac.cn

Research Article

Nitrogen and oxygen isotopes in nitrate and nitrite in the polluted surface waters from the Arno River Basin (Central Italy)

Lorenzo Chemeri [a,b,*], Barbara Nisi [c], Andrea Pierozzi [d], Jacopo Cabassi [c,e], Marco Taussi [a], Stefania Venturi [b,c,f], Antonio Delgado Huertas [g], Orlando Vaselli [b,c]

[a] Department of Pure and Applied Sciences, University of Urbino Carlo Bo, Via Ca' Le Suore 2/4, 61029, Urbino, Italy
[b] Department of Earth Sciences, University of Florence, Via G. La Pira 4, 50121, Florence, Italy
[c] Institute of Geosciences and Earth Resources (IGG), National Research Council of Italy (CNR), Via G. La Pira 4, 50121, Florence, Italy
[d] iCRAG, Department of Geology, School of Natural Sciences, Trinity College Dublin, Dublin, D02PN40, Ireland
[e] Istituto Nazionale di Geofisica e Vulcanologia (INGV), Sezione di Roma1, Via di Vigna Murata 605, 00143, Rome, Italy
[f] Istituto Nazionale di Geofisica e Vulcanologia (INGV), Sezione di Palermo, Via Ugo La Malfa 153, 90146, Palermo, Italy
[g] Laboratorio de Biogeoquimica de Isòtopos Estables, Instituto Andaluz de Ciencias de la Terra IACT (CSIC-UGR), Avda. de las Palmeras, 4, 18100, Armilla, Granada, Spain

ARTICLE INFO

Keywords:
River geochemistry
Water pollution
Nitrogen stable isotopes
Surface water management
Water quality
Anthropogenic pollution

ABSTRACT

The Arno River Basin (Central Italy) is affected by a considerable anthropogenic pressure due to the presence of large cities and widespread industrial and agricultural practices. In this work, 26 water samples from the Arno River and its main tributaries were analyzed to assess the water pollution status. The geochemical composition of the Arno River changes from the source (dominated by a Ca-HCO_3 facies) to the mouth (where a Na-Cl(SO_4) chemistry prevails) with an increasing quality deterioration, as suggested by the Chemical Water Quality Index, due to anthropogenic contributions and seawater intrusion before flowing into the Ligurian Sea. The Ombrone and Usciana tributaries introduce anthropogenic pollutants into the Arno River, whilst Elsa tributary supplies significant contents of geogenic sulfate. The concentrations of dissolved nitrate and nitrite (up to 63 and 9 mg/L, respectively) and the respective isotopic values of $\delta^{15}N$ and $\delta^{18}O$ were also determined to understand origin and fate of the N-species in the Arno River Basin surface waters. The combined application of $\delta^{15}N$-NO_3 and $\delta^{18}O$-NO_3 and N-source apportionment modelling allowed the identification of soil organic nitrogen and sewage and domestic wastes as primary sources for dissolved NO_3^-. The $\delta^{15}N$-NO_2 and $\delta^{18}O$-NO_2 values suggest that the nitrification process affects the ARB waters, thus controlling the abundances and proportion of the N-species. Our work indicates that additional efforts are needed to improve management strategies to reduce the release of nitrogenated species to the surface waters of the Arno River Basin, since little progress has been made from the early 2000s.

1. Introduction

Agricultural and industrial activities are regarded as the main responsible for the discharge of toxic pollutants (i.e., organic, inorganic, and/or biological) in natural environments, and river waters are extremely sensitive to anthropogenic contamination. Over the years, the influence of man-related activities, together with the effects produced by climate change, has affected both water quantity and quality (e.g., Di Matteo et al., 2017: Miller and Hutchins, 2017; Salerno et al., 2018; D'Oria et al., 2019; Gupta et al., 2021; Egidio et al., 2022). Nitrogen-bearing species (i.e., NO_3^-, NO_2^-, and NH_4^+) are considered to be among the main pollutants of surface waters and shallow aquifers at the global scale since these compounds are released by multiple sources like: (a) industrial discharges, (b) domestic waste, (c) agro-zootechnical wastes, (d) wastewater treatment, and (d) nitrogen fertilizers widely used in nursery and agricultural practices (Galloway et al., 2008; Capri et al., 2009; Nisi et al., 2013, 2022; Martinelli et al., 2018; Torres-Martínez et al., 2020, 2021; Abascal et al., 2022; Linhoff, 2022; Taussi et al., 2022). The contamination thresholds of NH_4^+ and NO_2^- (0.5 mg/L) are strictly regulated at national and European levels (e.g., Martínez-Navarrete et al., 2008; EU Directive, 2020/184/EC, 2020), since they are highly reactive compounds and turn into NO_3^- following the nitrification process (Andersson and Hooper, 1983). Molecular nitrogen can then be formed due to denitrification processes, mediated by bacterial activity which plays a key role in the whole nitrogen cycle (Kendall, 1998).

* Corresponding author.
E-mail address: l.chemeri@campus.uniurb.it (L. Chemeri).

https://doi.org/10.1016/j.jes.2025.03.064
Received 13 November 2024; Received in revised form 19 March 2025; Accepted 19 March 2025
Available online 28 March 2025

Nitrate represents the prominent nitrogen species in surface waters and a major nutrient. NO_3-excess can contribute to eutrophication (Schindler, 2006) often leading to aquatic ecosystems issues (Kharbush et al., 2023). Water consumption containing high levels of nitrate can cause serious health problems (Schullehner et al., 2018; Ward et al., 2018; Blaisdell et al., 2019), especially to children, for whom the maximum admissible nitrate content is 10 mg/L, i.e., five times lower with respect to the NO_3^- quality targeted for adult consumption (50 mg/L; Schullehner et al., 2018; EU Directive 2020/184/EC, 2020).

The first European Directive concerning nitrate pollution and management was enacted in 1991 (EU Directive 1991/676/ECC, 1991) and followed by the Water Framework Directive in 2000 (EU Directive 2000/60/EC, 2000), which was implemented in Italy by the Italian Law Decree 152/2006. The main objectives of these directives were to safeguard drinking water supplies and prevent eutrophication of fresh and marine waters (Martínez-Navarrete et al., 2008). Despite preservation and remediation actions, N-bearing compounds are still a major concern at small and large scales, whose origin is not always easy to be disentangled (Raco et al., 2021; Torres-Martínez et al., 2021; Abascal et al., 2022; Taussi et al., 2022, 2024).

In geochemical and environmental sciences, it is well established that nitrogen and oxygen isotopes in nitrate are useful tools to infer the primary source of nitrate in water systems, such rivers, lakes and aquifers (Clark and Fritz, 1997; Kendall, 1998; Fenech et al., 2012; Nisi et al., 2013; Divers et al., 2014; Matiatos, 2016; Sanchez et al., 2017; Zhang et al., 2019; Torres-Martínez et al., 2021; Matiatos et al., 2023). Furthermore, nitrate isotopes also provide clues on multiple reactions and complex dynamics that nitrate may undergo during transport which strongly influences its fate in water systems (Matiatos et al., 2021; 2023). These processes (e.g., nitrification, denitrification or volatilization) may act at different extent depending on the physical and chemical conditions (e.g., oxygen availability) sometimes leading to variations in the δ^{15}N-NO_3 and δ^{18}O-NO_3 values, thus hiding the pristine isotopic composition of the nitrate source. This represents a non-negligible problem when dealing with water management (Grimmeisen et al., 2017; Minet et al., 2017; Zhu et al., 2019; Torres-Martínez et al., 2021; Matiatos et al., 2023). Since the δ^{15}N-NO_3 values generally show overlapping ranges between different sources they do not allow to differentiate the primary source of nitrate (Mayer et al., 2002; Xue et al., 2009; Nisi et al., 2013; Minet et al., 2017; Zhu et al., 2019). Consequently, by combining δ^{15}N-NO_3 and δ^{18}O-NO_3 values, NO_3^- contents, and other major species (e.g., Na^+ and/or Cl^-), more precise constrains for defining the origin of dissolved NO_3^- can be envisaged (Roy et al., 1999; Torres-Martínez et al., 2021; Guo et al., 2020). Specifically, nitrate from synthetic fertilizers displays δ^{15}N values that are usually varying between −6 ‰ and +6 ‰ vs. AIR-NBS (Kendall, 1998; Xue et al., 2009), whilst those of δ^{18}O cluster around +23 ‰ vs. AIR-NBS. Contrarily, manure and sewage produce isotopically different nitrate, being generally enriched in the heavier isotope (^{15}N) (Choi et al., 2007) with a δ^{15}N signature varying from +5 ‰ to +25 ‰ vs. AIR-NBS (Clark and Fritz, 1997; Kendall, 1998) and δ^{18}O values below +15 ‰ vs. V-SMOW (Kendall, 1998; Torres-Martínez et al., 2021).

Contrarily, the determination of δ^{15}N-NO_2 and δ^{18}O-NO_2 is rarely carried out in surface and groundwater studies due to the high instability of nitrite, and it is usually focused on different environments (e.g., oceanic waters). Nitrite can form during nitrate reduction following the denitrification process while nitrification produces NO_2^- via ammonium and N oxidation. On the contrary, it can be consumed following nitrite reduction (to NO or N_2O) and oxidation (to NO_3^-) (Lewicka-Szczebak et al., 2021). During these processes, NO_2^- suffers isotopic fractionation (Buchwald and Casciotti, 2013; Denk et al., 2017; Lewicka-Szczebak et al., 2021). Hence, NO_2^- isotopes may provide useful clues to hypothesize their origin and sinks on active pathways in aqueous environment (Casciotti, 2009; 2016; Buchwald and Casciotti, 2010; Wells et al., 2016; Lewicka-Szczebak et al., 2021; Aharoni et al., 2022).

The Arno River Basin (hereafter, ARB) is one of the most important hydrological basins of Italy and is the eighth in terms of length. After the Tiber River Basin, the surface covered by ARB is the second one in Central Italy. Previous geochemical and isotopic studies revealed that water geochemistry is highly influenced by anthropogenic contributions, and critical contents of N-bearing species were evidenced (Nisi et al., 2005, 2008a). In fact, ARB is intensely urbanized as the Arno River flows through or close to large cities (e.g., Arezzo, Florence, Prato, Pisa), with most sub-basins hosting important industrial, agro-zootechnical, and nursery activities (Bencini and Malesani, 1993; Cortecci et al., 2002, 2009; Dinelli et al., 2005). According to Nisi et al. (2008b), the population in the ARB is of about 2.5 million people but the anthropogenic pressure is equivalent to 8.5 million inhabitants.

In this work, the chemical and isotopic results obtained from a sampling survey carried out in Autumn 2017 are reported, during which 26 waters were collected, 13 of which being sampled from the Arno River (AR) and 13 from its tributaries (T). The aims of this work were to (1) update the geochemical knowledge of the ARB surface waters and assess their quality status by applying the Chemical Water Quality Index (CWQI) (Chemeri et al., 2023), and (2) understand and constrain the origin and fate of N-bearing species in the ARB waters. For this purpose, nitrogen and oxygen stable isotopes were determined in both nitrate (δ^{15}N- and δ^{18}O-NO_3) and nitrite (δ^{15}N- and δ^{18}O-NO_2), the latter being the first measurements ever carried out in the Arno River catchment.

The N-bearing species concentrations were also compared to those determined in previous works in 2002–2003 by Nisi et al. (2005, 2008a) in order to highlight and assess their evolution over time. Finally, an evaluation of the remediation and preservation actions following the introduction of the Water Framework Directive (EU Directive 2000/60/EC, 2000) was also considered. This study represents a further step ahead in understanding the environmental status of one of the most important Italian river basins. It indeed provides helpful insights into the main nitrogen pollution sources by using the isotope systematics of nitrite and nitrate, allowing to design resolute actions to improve the management and quality of the Arno River Basin waters.

1.1. Geological, hydrological and anthropogenic background

ARB is located in Tuscany (98.4 %) and Umbria (1.6 %), Central Italy, and its hydrographic catchment covers an area of 8228 km^2 (Fig. 1) with an average elevation of 353 m a.s.l. The Arno River springs from the southern slope of Mt. Falterona, in the Northern Apennines, at the elevation of 1385 m (*Capo d'Arno* spring), flows for 242 km, also passing through the world heritage city of Florence, and ends its course in the Ligurian Sea, 10 km west of the city of Pisa (Fig. 1). The lithologies of the catchment are mainly composed of sedimentary folded and faulted Mesozoic and Tertiary units (Fig. 1a) (Abbate et al., 1992; Cortecci et al., 2002; Nisi et al., 2008a) that resulted from the formation of the Apennine Chain. The subsequent Pleistocene extensional tectonic phase created a NW-SE-oriented horst and graben system followed by the Arno River drainage network and consisting of six main sub-basins, namely: Casentino (CA), Chiana Valley (CH), Sieve (SI), Upper Valdarno (UV), Middle Valdarno (MV), Lower Valdarno (LV) (Fig. 1a) (Baldacci et al., 1967; Carmignani and Kligfield, 1990). The upper part of the ARB is dominated by sandstones (Cervarola and Macigno Fms), located in the source area, and marls (Pliocene continental and lacustrine deposits) in the Chiana Valley. Predominant sandstone lithologies also characterize the upper reaches of the Sieve sub-basin, although many springs feeding the Sieve River flow within calcareous facies belonging to the Ligurian Flysch (Cortecci et al., 2002; Nisi et al., 2008a). Downstream of Florence, the Bisenzio, Ombrone, and Usciana rivers (i.e., right-hand tributaries) flow within the Macigno Fm sandstones and, to a lesser extent, cherty limestones, whilst the left-hand tributaries, i.e., Greve, Pesa, Elsa, Egola, Era, drain Plio-Quaternary marine and lacustrine clayey and sandy deposits (Cortecci et al., 2002). The upper reaches of the Elsa and Era catchments are also characterized

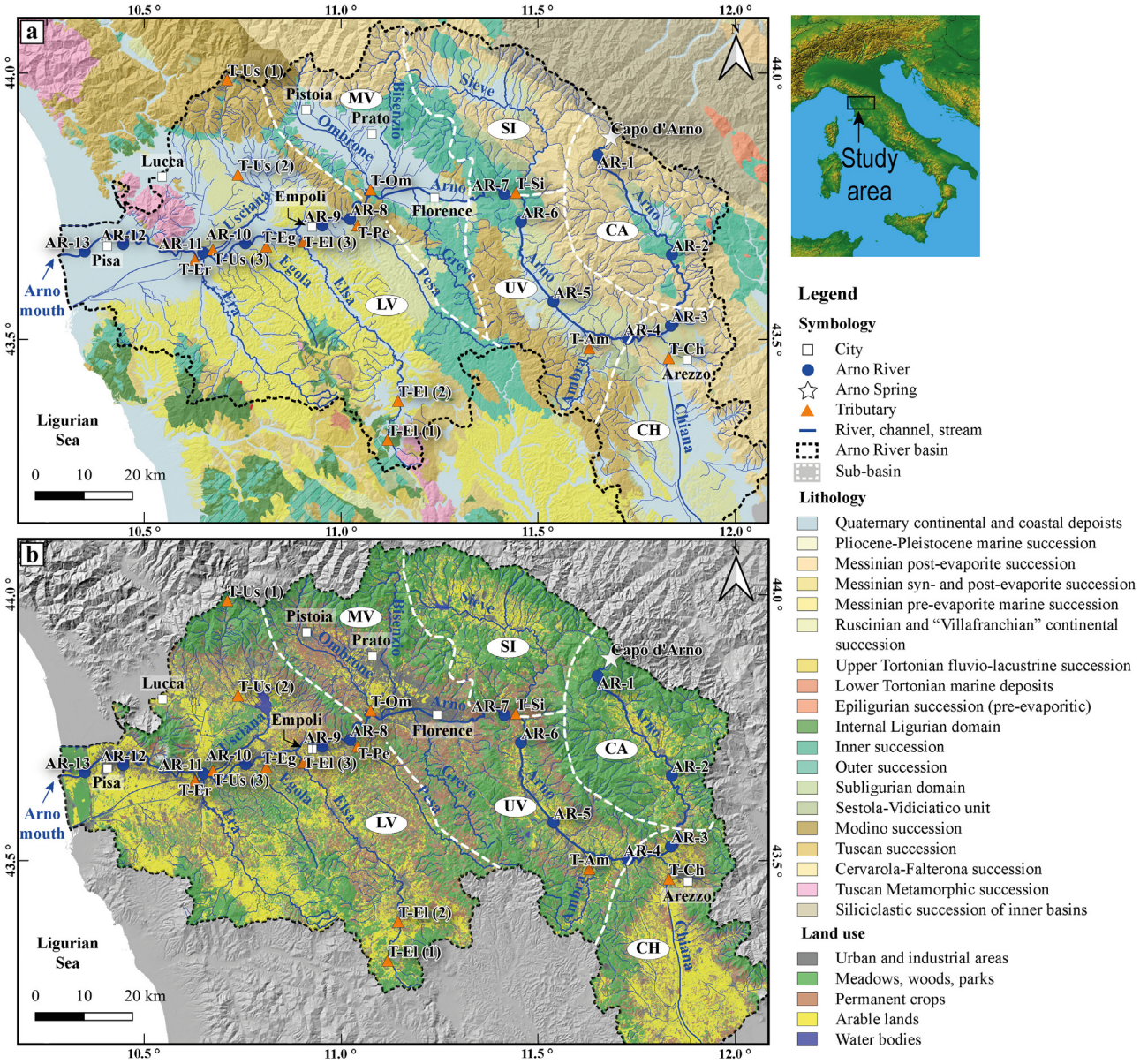

Fig. 1 – (a) Geological (after Conti et al., 2020) and (b) land use (after Regione Toscana, 2019) maps of the Arno River Basin (ARB) and locations of the sampling sites (IDs as reported in Table 1). The Arno River catchment is divided into six sub-basins, as follows: Casentino (CA), Chiana (CH), Sieve (SI), Upper Valdarno (UV), Middle Valdarno (MV) and Lower Valdarno (UV). The location of the Arno Spring (*Capo d'Arno*) and the main cities are also reported on the map.

by the outcrop of Triassic and Messinian evaporites. Finally, in the last part of its course, the Arno River flows in the coastal plain around Pisa which mainly consists of alluvial deposits (Cortecci et al., 2002, 2009; Nisi et al., 2008a). Notably, the Ambra and the Elsa tributaries are also interested by the discharge of thermo-mineral springs (T < 45 °C) in their main courses (Nisi et al., 2008a, 2008b).

Concerning the main hydrological features of the ARB, the rainfall regime is characterized by a precipitation peak in autumn (October and November, 140 mm), with a gradual decrease starting from January and a minimum in the summer months (July and August, >40 mm), with remarkable spatial variations in the distribution of precipitation due to the complex orography (Giani and Panichi, 2003 and references therein). The hydrometric regime of the river is highly variable, showing peaks in December (60 m^3/s) and minimum in August and September (>10 m^3/s). ARB has a distinctly torrential character before Arezzo, as it is characterized by a low storage capacity due to the presence of predominantly impermeable soils, especially in the sub-basins of the Sieve and Casentino (Fig. 1), which contribute most to the river flow (Giani and Panichi, 2003).

The Arno River meanders in a highly urbanized and human-developed area (Fig. 1b) that suffered more than a century of industrial and demographic development. Previous investigations highlighted the major anthropogenic inputs (Bencini and Malesani, 1993; Cortecci et al., 2002, 2009; Dinelli et al., 2005; Nisi et al., 2005, 2008a), as follows: (a) significant effects related to the anthropogenic pressure resulting from the confluence with the Chiana tributary since the main course receives untreated wastewaters produced by agricultural and zoo-technical activities; (b) discharge of domestic black and white water systems (after partial cleaning by purifier plant systems) by the city of Florence; (c) release by the Bisenzio and Ombrone tributaries of wastewaters produced from industrial (mostly textile) and nursery activities located around the cities of Prato and Pistoia; (d) tanneries and paper-mills discharge upstream from Pisa, such as the partly-treated waters from the Usciana channel and other minor tributaries (Tognotti et al., 1998) and, eventu-

Table 1 – List of the sampling points. ID, full name of the sampling location, sampled river, geographic location (in UTM-WGS84 coordinates), pH, T, and electrical conductivity (EC) are reported.

ID	Sampling location (river)	UTM North	UTM East	pH	T (°C)	EC (μS/cm)
AR-1	La Casina (*Arno*)	4857687	713493	7.80	9.6	306
AR-2	Rassina (Arno)	4837145	728797	8.05	13.0	528
AR-3	Buon Riposo (*Arno*)	4822514	728625	7.54	16.7	426
AR-4	Laterina (*Arno*)	4819,786	719774	7.80	18.5	729
AR-5	S. Giovanni Vald. (*Arno*)	4827489	704380	7.89	19.2	756
AR-6	Rignano (*Arno*)	4843954	697701	8.00	18.2	769
AR-7	Rosano (*Arno*)	4849623	694283	8.32	17.7	668
AR-8	Montelupo (*Arno*)	4844503	662471	7.78	11.8	1041
AR-9	Empoli (*Arno*)	4843168	656740	7.86	11.4	1026
AR-10	Castelfranco di Sotto (*Arno*)	4839481	640886	8.10	14.9	1636
AR-11	Ponte alla Navetta (*Arno*)	4837548	632185	8.48	14.4	1792
AR-12	Pisa (*Arno*)	4839325	615688	7.63	10.7	5450
AR-13	Marina di Pisa (*Arno*)	4837811	607752	7.76	11.5	12,720
T-Ch	P. ai Chiani (*Chiana*)	4815845	728172	7.26	17.3	1445
T-Am	Bucine (*Ambra*)	4817919	711771	8.14	17.4	2190
T-Si	Pontassieve (*Sieve*)	4849926	696646	8.25	18.3	653
T-Om	Comeana (*Ombrone*)	4850575	666673	7.76	14.0	2340
T-Pe	Montelupo (*Pesa*)	4843186	663994	7.97	12.1	840
T-El (1)	Molino d'Elsa (*Elsa*)	4798982	670194	7.85	12.7	922
T-El (2)	Onci (*Elsa*)	4807036	672361	7.57	18.5	2980
T-El (3)	P. a Elsa (*Elsa*)	4839849	652795	8.12	10.8	1838
T-Eg	P. a Egola (*Egola*)	4838857	645173	7.60	10.0	1166
T-Us (1)	Stiappa (*Usciana*)	4873235	637125	7.59	10.0	240
T-Us (2)	Vione (*Usciana*)	4853649	639327	7.49	14.5	1080
T-Us (3)	Montecalvoli (*Usciana*)	4838208	634182	7.58	15.6	7440
T-Er	Pontedera (*Era*)	4836125	630470	7.81	11.5	1282

ally (e) intrusion by seawater that affects the Arno River in its final part. West winds may occasionally extend the effects of the saline wedge up to 27 km toward the inland (Bencini and Malesani, 1993; Cortecci et al., 2002; Nisi et al., 2005; 2008a).

2. Materials and methods

2.1. Chemical and isotopic analysis

In autumn 2017, 26 waters were collected (Table 1): (1) 13 samples from the Arno River (AR-1 to AR-13) to cover the entire length of the main course from close to its source to few kms before entering the sea, and (2) 13 samples from the Arno river major tributaries before their confluence with the main course, namely Chiana (T-Ch), Ambra (T-Am), Sieve (T-Si), Ombrone (T-Om), Pesa (T-Pe), Elsa (T-El), Egola (T-Eg), Usciana (T-Us) and Era (T-Er). Additionally, the T-El and T-Us were sampled at three different points locations along the rivers' course (Fig. 1). The sampling strategy was meant to cover as much as possible the entire basin to provide a comprehensive overview of the river environmental status and the factors influencing it such as (a) land-use and presence of industrial activity, (b) confluence of the tributaries and (c) geological and physical characteristics of the different sub-basins.

The waters were collected from the central part of the river to avoid the so-called "bank effect". Temperature, pH, and electrical conductivity (EC) were determined in situ using a Crison 2000 multiparametric probe (Table 1). At each sampling point, three different aliquots were collected as follows: (a) one unfiltered 250 mL polyethylene (PE) bottle for the analysis of the main anions and N-bearing species, (b) one filtered (0.45 μm) and pre-acidified (with 1 % Suprapur HCl) 50 mL PE bottle for the analysis of the main cations, and (c) eight not filtered 12 mL glass vials containing 0.5 mg of $HgCl_2$ for the isotopic analysis of carbon and nitrogen and oxygen in the total dissolved inorganic carbon (TDIC) and NO_2 and NO_3, respectively. The addition of $HgCl_2$ removes any effect by microbial activity avoiding any possible fractionation processes after sample collection (Atekwana et al., 1998). The water samples were stored at +4 °C before the isotopic analysis. Total alkalinity (as HCO_3^-) was analyzed by acidimetric titration (AT) using an automatic burette filled with 0.01 M HCl and methyl-orange as an indicator. The main anions (Cl^-, SO_4^{2-}, Br^-, F^-, NO_3^-) and cations (Ca^{2+}, Mg^{2+}, Na^+, K^+) were determined by ion chromatography (IC), using Metrohm 761 Advanced Compact IC and Metrohm 861 Compact IC chromatographs, respectively. Nitrite (NO_2^-) and ammonia (NH_4^+) were analyzed, within 24 h from collection, by molecular spectrophotometry (MSP) using a HACH DR2010 instrument. The analytical errors for AT, IC, and MSP were below 5 % (Chemeri et al., 2024). The analysis of δ^{13}C-TDIC was carried out following the method described by Salata et al. (2000), where the CO_2, extracted from the solution following the interaction with anhydrous phosphoric acid (H_3PO_4), was analyzed with a Finnigan Delta Plus X mass spectrometer. Finally, the isotopic analysis of δ^{15}N and δ^{18}O in NO_2^- and NO_3^- was carried out using a Finnigan V Plus mass spectrometer according to the method proposed by McIlvin and Altabet (2005). The experimental error for δ^{13}C-TDIC was ±0.1 ‰ vs. V-PDB while it was within ±0.3 ‰ vs. Air-NBS for both δ^{15}N and δ^{18}O in nitrate and nitrite. The accuracy and precision of the isotopic analyses were confirmed using 3 internals standards of Na_2CO_3 solution (DIC-A, DIC-B and DIC-T), each with a different carbon isotopic composition (−4.9 ‰, −9.50 ‰, +28.59 ‰ vs. V-PDB) and compared with the IAEA international references NBS-18, NBS-19, NBS-20 (for carbonates) and NBS-22, IAEA-CH-7, IAEA-CH-6, USGS-61, USGS-62 (for organic material) for TDIC samples. For the N-bearing species, the international standards IAEA-N3, USGS-34 and USGS-35 were used as reference materials. The standard deviation for both methods was below 0.01 ‰. For more details on the analytical procedure, we refer to the afore-mentioned papers (Salata et al., 2000; McIlvin and Altabet, 2005).

All water chemical analyses were performed at the Laboratory of Fluid Geochemistry of the Department of Earth Sciences of the University of Florence, Italy, whilst the isotopic analyses were carried out at the Laboratory of Stable Isotopes Biogeochemistry at the Andalusian Institute of Earth Sciences (IACT) in Granada, Spain.

2.2. Water quality indexing and EMMTE approach for nitrate source contributions

The quality status of the ARB running waters was determined using the Chemical Water Quality Index (CWQI) computation reported in Chemeri et al. (2023). The CWQI is a multi-parametric weighted water

quality index that allows to estimate the quality status of any type of water in every kind of environment. The CWQI was chosen since it presents strong advantages compared to the other indexes available in the literature (Uddin et al., 2021): (1) the inclusivity of the variables, since any parameter can be considered in the index computation, differently to most of the available WQIs (Kachroud et al., 2019; Uddin et al., 2021); (2) the simple and unbiased weightage method, and (3) the universal applicability without limitations due to site-specificity and water-body dependance (Chemeri et al., 2023). The CWQI computation is divided into two phases. The first step selects the variables to be included; since they may be reported on different scales, a parametrization phase is required. The choice of the variables is at the user's discretion. The parametrization consists in assigning a score (s) from 1 to 10 to each variable based on the measured value/concentration and quality targets ratios, in our case represented by EU Directive 2020/184/EC (2020). Consequently, a weight (w) directly proportional to the score (s) is assigned to each variable. The weightage method gives the parameter a relative importance that only depends on the concentration of that parameter with respect to its quality target. Hence, the weights are determined every time a new water is tested. The final step is the index computation in which all the single scores and weights are aggregated together (using a multiplicative aggregation formula) producing a single number that summarizes the overall water quality status.

The contribution of a single species or compound to the water quality can be reported as influence (or impact) factor (IF_x) which is given by the sum of the weights (w_i) recalculated to one hundred (%) according to Eq. (1).

$$IF_x = 100 \times w_x = 100 \times \frac{S_x}{\sum_{i=1}^{n} S_i} \quad (1)$$

where, w_x is the weight of the parameter x, S_x is the score of the parameter x and the denominator is the sum of the scores including all the variables taken into account by Chemeri et al. (2023).

The proportional contributions of the possible NO_3^- pollution sources were determined using the EMMTE approach, i.e., an end-member mixing model tool on Excel, developed by Cao et al. (2023). This methodology was chosen since it can be easily run on an Excel spreadsheet and the results provided are consistent with the MixSIAR models (Cao et al., 2023; Shi et al., 2024). In our case, we considered the dual-isotopic nitrate values (δ^{15}N- and δ^{18}O-NO_3) and four potential sources in the study area: atmospheric deposition (AD), sewage and manure (SM), soil organic nitrogen (SON) and chemical fertilizers (CF). The different end-member isotopic compositions were defined based on previously published literature (Fenech et al., 2012; Torres-Martinez et al., 2021; Cao et al., 2023), as follows: AD ($\delta^{15}N_{NO3}$: +0.11 ‰, $\delta^{18}O_{NO3}$: +54.97); CF ($\delta^{15}N_{NO3}$: −0.37 ‰, $\delta^{18}O_{NO3}$: +2.87 ‰), SON ($\delta^{15}N_{NO3}$: +2.36 ‰, $\delta^{18}O_{NO3}$: −3.59 ‰) and MS ($\delta^{15}N_{NO3}$: +10.4 ‰, $\delta^{18}O_{NO3}$: +5.69 ‰). It is important to note that the results obtained through this method, as well as those achieved using MixSIAR models, may have some limitations. In fact, they do not fully consider the multiple processes that surface waters may undergo within the catchment (i.e., water-atmosphere exchanges and/or interactions with soil and stream sediments) that are difficult to be quantified and may notably alter the chemical and isotopic composition of surface waters.

3. Results

3.1. Water geochemical features

The physicochemical data and the concentrations of the main cations, anions and nitrogenated species are listed in Table 1 and Table 2, respectively. The pH ranged from 7.20 to 8.48, with most waters showing a slightly alkaline pH, whilst temperature was comprised between 9.6 and 19.2 °C. Total Dissolved Solids (TDS, expressed as the sum, in mg/L, of the main ions) increased along the river course, moving from AR-1 (the closest sampling site to the Arno River spring), being characterized by a TDS of 226 mg/L, to AR-13 (collected a few km before the Ligurian Sea) with a TDS of 7710 mg/L. Among the tributaries, the lowest and highest TDS values pertained to the Usciana River, being T-Us (1) and T-Us (3) characterized by 157 and 5047 mg/L, respectively.

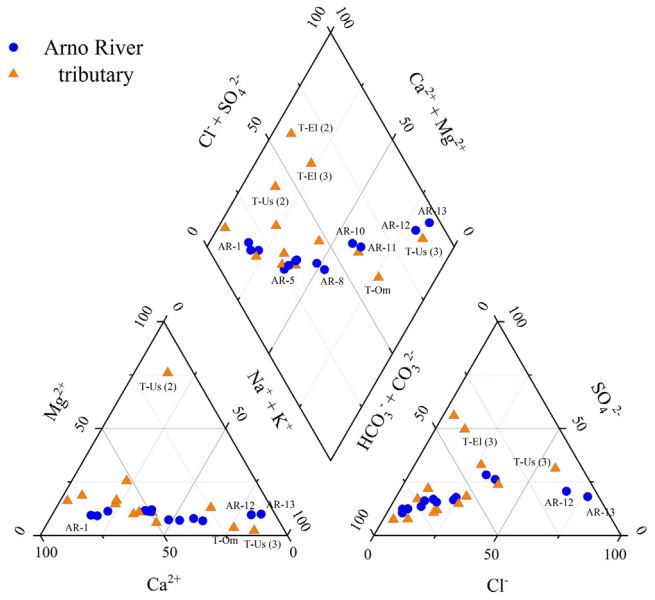

Fig. 2 – Piper classification diagram for the ARB running waters. IDs as reported in Table 1.

According to the main ion abundances, the ARB waters can be classified (Fig. 2) as mainly dominated by a Ca-HCO_3 facies (most waters from the main course (AR-1 to AR-9) and tributaries (T-Ch, T-Si, T-Pe, T-Eg, T-El (1), T-Us (2), T-Us (1)). Differently, Na-Cl waters refer to the final segment of the Arno River (Lower Valdarno: AR-10 to AR-13) and those of T-Om and T-Us (3), being characterized by Na^+ and Cl^- contents up to 2235 mg/L and 3280 mg/L, respectively. Finally, a SO_4-rich component characterizes T-Am, T-El (2) and T-El (3), which display a Na-SO_4(Cl) and Ca-SO_4 geochemical facies, respectively (Table 2).

Bromide showed variable contents along the Arno River course from below the limit of detection (0.01 mg/L) up to 15.0 mg/L (Table 2), the highest values being found close to the Arno River mouth (i.e., AR-12 and AR-13). Fluoride spanned from 0.1 (AR-1, AR-2, AR.3 and T-Us (1)) to 5.6 mg/L (T-Us (3)). As far as the N-bearing species are concerned, NO_3^- was comprised between 0.82 (AR-1) and 62.5 mg/L (T-Us (3)), NO_2^- ranged between 0.01 (T-Pe, T-El (2)) and 8.72 mg/L (T-Er), and NH_4^+ spanned from 0.03 (AR-1, AR-2) to 4.77 mg/L (T-Us (3)).

The chemical quality status of the waters, computed according to the CWQI, was applied by considering pH, EC, F^-, Cl^-, NO_3^-, NO_2^-, SO_4^{2-}, Na^+, hardness (as a function of Ca^{2+} and Mg^{2+}), and NH_4^+ using the European quality standards for drinking waters as reference values (EU Directive 2020/184/EC, 2020). The CWQI values span from 1.17 to 9.12 and increase from AR-1 to AR-13 (Table 2), i.e., from good to extremely poor water quality. The Arno River tributaries show a relatively large CWQI variability. Few of them (e.g., T-Si, T-Eg, T-Ch, T-Pe) have indeed values below 4 (a good to medium quality status) whereas others (e.g., T-Om, T-El (3), T-Us (3)) are up to > 5, indicating poor water quality.

3.2. Nitrogen and carbon isotopic composition

The δ^{15}N and δ^{18}O values (reported as ‰ vs. Air-NBS and ‰ vs. V-SMOW, respectively) in nitrate and nitrite and those of δ^{13}C-TDIC (expressed as ‰ vs. V-PDB), are reported in Table 3. The δ^{13}C-TDIC values showed relatively negative values spanning between −14.5 ‰ (T-Om) and −0.5 ‰ (T-Am). All the δ^{15}N-NO_3 values were positive (up to +18.5 ‰ vs. Air-NBS, T-Ch) with the only exception of T-Eg (−5.1 ‰). Con-

Table 2 – Major (alkalinity as HCO_3^-, chloride, nitrate, sulfate, calcium, magnesium, sodium, and potassium), minor (fluoride, bromide, nitrite, and ammonia), and TDS (total dissolved solids, given by the sum of major and minor components contents) are reported in mg/L.

ID	Alkalinity	F	Cl	Br	NO_3	NO_2	SO_4	Ca	Mg	Na	K	NH_4	TDS	CWQI	Rank
AR-1	140	0.1	9	0.01	0.8	0.02	21	41	5	8	1.2	0.03	226	1.18	G
AR-2	253	0.1	19	0.13	3.3	0.03	32	76	10	17	2.4	0.03	413	1.51	G
AR-3	224	0.1	21	0.13	3.9	0.03	35	65	11	19	2.1	0.06	381	1.49	G
AR-4	248	0.4	65	0.20	8.0	0.09	58	67	15	48	5.1	0.13	515	1.76	G
AR-5	246	0.2	41	0.10	4.1	0.07	45	67	15	43	4.2	0.10	466	1.66	G
AR-6	235	0.2	54	0.10	9.2	0.11	59	69	17	50	5.2	0.14	499	1.79	G
AR-7	242	0.2	42	0.11	6.6	0.05	55	67	15	44	4.9	0.13	477	1.89	G
AR-8	292	0.4	123	bdl	16.0	6.49	90	91	16	113	7.0	0.10	755	4.00	F
AR-9	276	0.5	111	bdl	20.5	6.56	77	91	15	92	7.1	0.12	697	3.92	F
AR-10	331	0.6	256	0.25	26.3	0.81	232	128	30	203	16.0	0.06	1224	4.76	P
AR-11	336	1.3	320	0.40	24.0	0.40	233	125	28	239	14.0	0.28	1321	4.81	P
AR-12	239	0.7	1372	5.00	10.5	4.14	419	107	106	851	31.0	0.16	3146	8.28	Ep
AR-13	220	4.6	3823	15.0	5.0	0.91	894	155	275	2235	82.0	0.18	7710	8.47	Ep
T-Ch	462	0.6	131	0.27	6.5	0.03	81	136	29	105	5.5	0.13	957	2.98	F
T-Am	393	0.3	264	0.29	8.3	0.06	324	109	58	265	14.0	0.10	1436	4.88	P
T-Si	251	0.3	31	0.04	6.6	0.05	58	60	12	35	3.1	0.06	457	1.63	G
T-Om	372	1.5	378	bdl	15.0	7.41	234	100	18	371	15.0	0.17	1512	6.00	P
T-Pe	303	0.3	81	bdl	8.2	0.01	46	103	18	55	4.0	0.08	619	2.09	F
T-El (1)	440	0.4	53	bdl	9.8	0.03	41	94	46	37	3.0	0.05	724	2.50	F
T-El (2)	519	3.8	58	1.00	2.0	0.01	734	365	92	34	4.0	0.06	1813	5.75	P
T-El (3)	415	2.5	129	bdl	18.1	4.03	536	255	69	79	16.0	0.45	1524	6.11	Vp
T-Eg	392	2.0	64	bdl	2.3	0.04	128	135	32	41	9.0	0.14	805	2.91	F
T-Us (1)	106	0.1	5	0.01	bdl	0.02	9	30	6	1	0.1	0.10	157	1.17	G
T-Us (2)	220	0.3	101	1.11	29.8	4.10	56	10	73	13	0.1	1.80	510	5.54	P
T-Us (3)	349	5.6	1839	2.90	62.5	1.18	995	220	41	1473	53.0	4.77	5047	9.12	Ep
T-Er	307	0.6	163	3.00	20.5	8.72	105	135	16	111	8.0	0.12	878	4.40	P

The Chemical Water Quality Index (CWQI) and the quality rank, i.e., G: good (CWQI < 2); F: fair (2.01 < CWQI < 4); P: poor (4.01 < CWQI < 6); Vp: very poor (6.01 < CWQI < 8); Ep: extremely poor (CWQI > 8.01), according to Chemeri et al. (2023), are also reported. "bdl" indicates values below the detection limit.

Table 3 – δ^{15}N (‰ vs. Air-NBS) and δ^{18}O (‰ vs. V-SMOW) values in nitrate and nitrite, and those of δ^{13}C-TDIC (‰ vs. V-PDB).

ID	δ^{15}N-NO_3	δ^{18}O-NO_3	δ^{15}N-NO_2	δ^{18}O-NO_2	δ^{13}C-TDIC
AR-1	n.d.	n.d.	n.d.	n.d.	−8.1
AR-2	13.9	−1.5	n.d.	n.d.	−8.7
AR-3	10.8	0.2	n.d.	n.d.	−8.0
AR-4	5.4	−2.2	n.d.	n.d.	−5.7
AR-5	8.1	−0.4	−0.8	2.4	−6.3
AR-6	10.2	−2.4	2.5	3.7	−7.0
AR-7	16.7	−3.7	3.6	5.2	−6.9
AR-8	10.5	−1.6	0.2	0.0	−11.3
AR-9	9.4	−3.6	−2.3	−0.9	−11.0
AR-10	14.8	2.3	2.6	−0.9	−8.8
AR-11	14.2	2.1	1.4	0.1	−7.4
AR-12	6.5	0.3	−2.9	−1.6	−10.8
AR-13	5.7	−0.6	−2.2	−2.7	−8.9
T-Ch	18.5	3.6	n.d.	n.d.	−6.3
T-Am	8.8	−2.2	−3.8	3.9	−0.5
T-Si	n.d.	n.d.	−0.5	4.8	−8.1
T-Om	5.9	−0.5	−6.8	−4.9	−14.5
T-Pe	18.1	3.3	n.d.	n.d.	−8.8
T-El (1)	9.2	0.3	11.3	3.6	−13.5
T-El (2)	n.d.	n.d.	n.d.	n.d.	−0.7
T-El (3)	4.2	−2.8	−0.5	−3.9	−6.0
T-Eg	−5.1	−4.4	−10.3	3.4	−12.7
T-Us (1)	n.d.	n.d.	n.d.	n.d.	−11.9
T-Us (2)	7.4	−0.7	−8.1	0.5	−13.1
T-Us (3)	8.5	1.2	−2.6	−1.4	−12.0
T-Er	4.5	−2.2	−7.5	−2.2	−10.2

n.d.: not determined due to low concentrations.

trarily, the δ^{18}O-NO_3 values were comprised in a narrower range, from −4.3 ‰ (T-Eg) to +3.6 (T-Ch) ‰ vs. V-SMOW. The δ^{15}N-NO_2 values were ranging from −10.3 ‰ (T-Eg) to +11.3 ‰ (T-El (1)) vs. Air-NBS, whilst those of δ^{18}O-NO_2 were included between −4.9 ‰ (T-Om) and +5.2 ‰ (AR-7) vs. V-SMOW. It is to be noted that due to very low concentrations, the isotopic values of nitrogen and oxygen of nitrate and nitrite could not be determined in a few samples (Table 3). The relationships between δ^{15}N-NO_3 and δ^{18}O-NO_3 values vs. NO_3^- contents and those of δ^{15}N-NO_2 and δ^{18}O-NO_2 vs. NO_2^- concentrations are reported in the supplementary materials (Appendix A Fig. S1). In Appendix A Fig. S1a, the δ^{15}N-NO_3 values are reported against the NO_3^- contents where three trends can be recognized: (i) large variability of the δ^{15}N-NO_3 values for most water samples characterized by low NO_3^- concentrations (< 10 mg/L) (i.e., AR-2, AR-3, AR-4, AR-5, AR-6, AR-7. AR-13, T-Ch, T-Am, T-Pe), spanning from +5.4 ‰ up to +18.5 ‰ vs. Air-NBS; (ii) increase of the nitrogen isotopic ratio and that of the NO_3^- contents (i.e., AR-8, AR-9, AR-10, AR-11, AR-12); and (iii) minimal variability of the δ^{15}N-NO_3 values at increasing nitrate abundance (i.e., T-Om, T-El (3), T-Us (2), T-Er). These trends are less evident when the δ^{18}O-NO_3 values vs. NO_3^- contents are considered (Appendix A Fig. S1b). As far as the δ^{15}N-NO_2 ratios vs. NO_2^- contents are concerned (Appendix A Fig. S1c), a general decreasing trend of the nitrogen isotopes at increasing NO_2^- concentrations is highlighted, especially for those waters characterized by high NO_2^- (> 1 mg/L) (e.g., T-Om, T-Us (2), T-Er), which is also observable when δ^{18}O-NO_2 vs. NO_2^- concentrations are considered (Appendix A Fig. S1d).

4. Discussion

4.1. Processes governing surface water geochemistry

The large compositional variability detected in the ARB waters is a consequence of different processes including both geogenic and anthropogenic sources. Along the Arno River, from AR-1 to AR-13, a progressive change from low to medium saline Ca(Mg)-HCO_3 waters towards a highly saline Na-Cl(SO_4) composition is highlighted (Fig. 2). This evolutionary trend is also associated with an increase of the CWQI that grows from 1.18 (AR-1) to 8.47 (AR-13), unequivocally suggesting a gradual deterioration of the water quality. Compositional changes as well as the TDS values are indeed related to (a) increasing water-rock interactions processes throughout the main course, (b) inputs deriving from anthro-

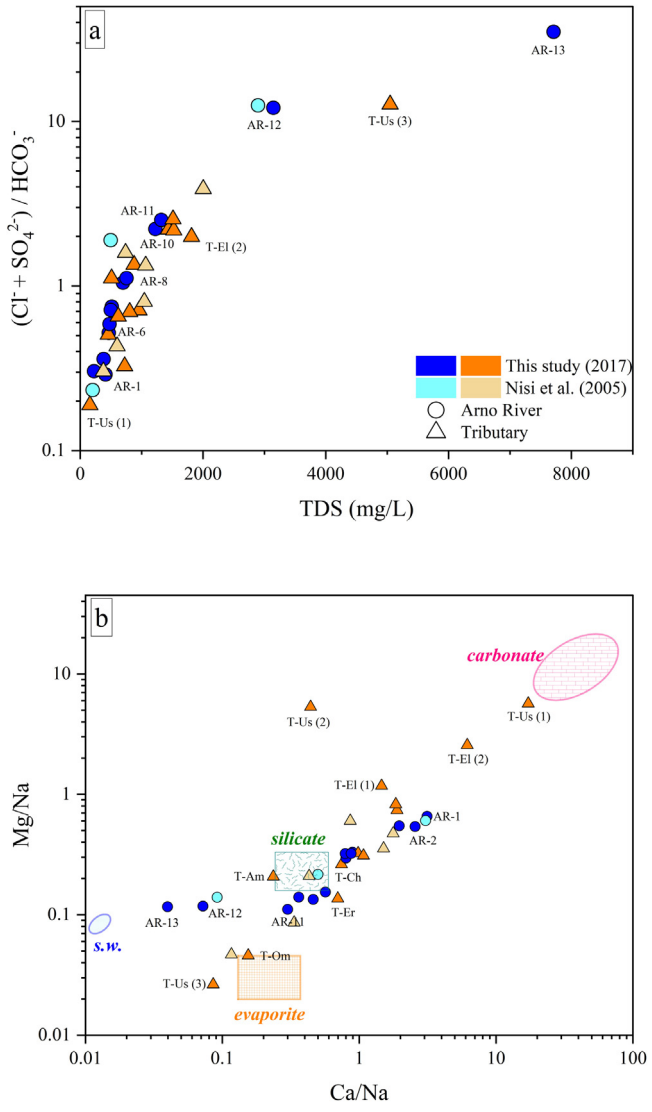

Fig. 3 – (a) $(Cl^- + SO_4^{2-})/HCO_3^-$ vs. total dissolved solids (TDS), reported in molar ratios and mg/L respectively, for the investigated waters; (b) Mg/Na vs. Ca/Na, values are in molar ratios, the evaporite, silicates, carbonates and seawater fields are reported after Gaillardet et al. (1997). Data from Nisi et al. (2005) are also reported for comparison. IDs as reported in Table 1.

pogenic activities, and (c) occurrence of seawater intrusion in the final part of the Arno River course (Fig. 2).

The Ca-HCO_3 waters from ARB dominate the reaches upstream of AR-9 (sampled close to Empoli, Fig. 1), while downstream the Na-Cl component becomes predominant with a $(Cl^-+SO_4^{2-})/HCO_3^-$ ratio gradually increasing with the TDS (Fig. 3a). The Ca-HCO_3 waters are the consequence of carbonate minerals dissolution (mainly calcite and minor dolomite), but they also show slight enrichments in earth alkaline ions with respect to bicarbonate, indicating the occurrence of alteration processes involving other mineral phases (Fig. 3b), e.g., Al-silicates. This is consistent with the ARB lithologies since the main course and its tributaries mainly drain silicate and carbonate rocks and, to a lesser extent, evaporites (Cortecci et al., 2002, 2007; Nisi et al., 2008a; Fig. 1a). The Arno River samples collected near the mouth (AR-12 and AR-13) are aligned toward the seawater end-member (Fig. 3b), indicating a clear contribution from seawater intrusion (Giani and Panichi, 2003; Nisi et al., 2008a). It is also worth mentioning that the Ombrone (T-Om) and Usciana (T-Us (3)) tributaries are distributed close to the evaporite dissolution field (Fig. 3b). Since no evaporitic lithologies are outcropping in the area (Fig. 1a), the Na^+ and Cl^- enrichments are related to anthropogenic inputs (Bencini and Malesani, 1993; Cortecci et al., 2002, 2009; Nisi et al., 2008a), which strongly endanger the water conditions, both tributaries showing a poor quality as supported by high CWQI values (6.0 and 9.1, respectively) (Table 2; Fig. 4). Additionally, it has to be considered that the Ambra (T-Am) and Elsa (T-El (2) and T-El (3)) tributaries, with the latter being characterized by $SO_4^{2-} >> Cl^-$, are partly fed by Ca-SO_4 thermo-mineral spring (T up to 45 °C), which represent the typical geochemical facies of most Tuscan thermal waters, related to fluids circulating at depth and interacting with the Triassic anhydrite formation, namely the Burano Fm (Minissale, 2004 and reference therein).

As far as the δ^{13}C-TDIC values are concerned, relatively negative values are recorded in the ARB waters (between −14.5 ‰ (T-Om) and −5.7 ‰ (AR-4) vs. V-PDB), indicating the dissolution of calcite and the interaction with biogenic soil CO_2 as the primary source for the carbon species (Chiodini et al., 2000; Grassa et al., 2006). Differently, T-Am and T-El (2) waters have δ^{13}C-TDIC values of −0.5 ‰ and −0.7 ‰ vs. V-PDB respectively, suggesting the interaction with an isotopically heavier CO_2 related to either (i) open carbonate system equilibration between TDIC and atmospheric CO_2 (Barth et al., 2003; Bottrell et al., 2019) or, more likely, (ii) the influence of a thermal component associated with the presence of CO_2-rich thermo-mineral springs in the ARB (Cortecci et al., 2002; Minissale, 2004; Nisi et al., 2008a). The δ^{13}C-TDIC values reported by Nisi et al. (2008b) and those of the present work are in good agreement, though slightly less negative (on average −9.00 ‰ vs. −10.3 %), with the exception of T-Ch (−6.3 ‰ vs. −10.6 ‰) and T-Am (−0.5 ‰ vs. −4.3 ‰). However, the δ^{13}C-TDIC evolution with respect to the distance from the source does not show significant variations for both surveys (Appendix A Fig. S2), suggesting analogous sources for the dissolved inorganic carbon.

Despite the fact that almost 15 years have passed since the last geochemical investigation carried out in the ARB by Nisi et al. (2005, 2008a), the ARB surface waters have similar features and comparable ion abundances (Fig. 4), confirming the findings already reported in the early nineties (Bencini and Malesani, 1993; Cortecci et al., 2002, 2009). In 2003 (Nisi et al., 2005) and 2017 (this work), the quality status of the ARB running waters was mainly controlled (and compromised) by the relatively high abundances of chloride (Fig. 4a) and sodium (Fig. 4b), and, subordinately, sulfate (Appendix A Fig. S3), with a strong increase in the Na-Cl component downstream from Florence with CWQI values above 4 (poor or worse). The first inputs of anthropogenically derived Na-Cl(SO_4) in the Arno River are recorded at the confluence of the Chiana (T-Ch) tributary and associated with the presence of agro-zootechnical activities (e.g., Cortecci et al., 2002; Nisi et al., 2008a). The major contributions in Na^+ and Cl^- are from the Ombrone (T-Om) and Usciana (T-Us (3)) tributaries discharge into the main course (Fig. 4a, b). Both tributaries are indeed flowing through areas where widespread nursery, tannery and industrial activities occur (Fig. 1b). As reported by Cortecci et al. (2002), the Bisenzio River, another right tributary (not analyzed in this study) of the Arno River, represents an additional source of anthropogenic-derived Na^+ and Cl^-, related to agricultural practices and nurseries, though to a minor extent with respect to T-Om and T-Us (3). The SO_4^{2-} contents exceeding the law limit (536 mg/L vs. 250 mg/L) at Elsa (T-El) tributary, strongly deteriorates the water quality (CWQI = 6.11, i.e., very poor), and although its origin is geogenic (Cortecci et al., 2002, 2007), its confluence in the Arno River represents an additional worsening factor in terms of quality (Figs. 4b and Appendix A Fig. S3). Contrarily, the Sieve (T-Si), Pesa (T-Pe), Egola (T-Eg), and Era (T-Er) tributaries are characterized by a good to fair quality status (Table 2) and they carry waters rich in Ca^{2+} (and Mg^{2+}) and carbonate species in the Arno River (Cortecci et al., 2002, 2007; Nisi et al., 2008a). Finally, approaching the Arno River mouth, seawater intrusion become the main process governing water composition, irreversibly compromising its quality (CWQI > 8, i.e., extremely poor).

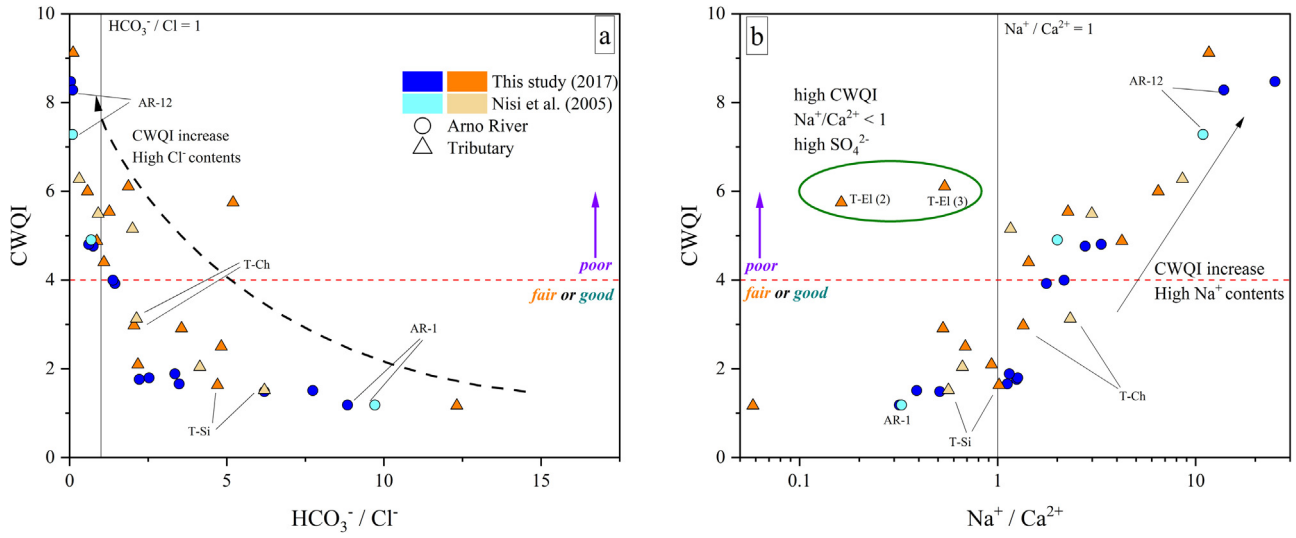

Fig. 4 – (a) CWQI vs. HCO_3^-/Cl^- and (b) CWQI vs. Na^+/Ca^{2+}diagrams for the waters sampled in 2003 (from Nisi et al., 2005) and 2017 (this study) surveys. HCO_3^-/Cl^- and Na^+/Ca^{2+} are reported as molar ratios. The horizontal red dashed lines, indicating the border between good/fair and poor water quality (after Chemeri et al. 2023), are also drawn. IDs as reported in Table 1.

4.2. Origin and fate of N-bearing compounds

On average, the ARB waters are characterized by $NO_3^- > NO_2^- \geq NH_4^+$, as expected in oxidizing environments, where NH_4^+ is extremely reactive and unstable and tends to form NO_3^-, following the nitrification process, with NO_2^- as an intermediate product. The concentrations of NO_3^- in the ARB surface waters were below the quality target for all samples with the exception of T-Us (3) (62.5 mg/L), whilst NO_2^- did not meet the quality target in ten samples with a few waters exceeding up to more than ten times the law limit (e.g., T-Om, 7.41 mg/L; T-Er, 8.72 mg/L). Critical NO_3^- contents pertain to the Lower Valdarno sub-basin whilst high NO_2^- concentrations characterize the Middle and Lower Valdarno. Ammonium exceeded the quality target in T-Us (2) and T-Us (3), the latter showing NH_4^+ content of 4.77 mg/L, i.e., almost ten times higher than the limit imposed by the EU Directive.

When compared to the values reported by Nisi et al. (2005), nitrate contents are similar in the two different periods with an average of 9.6 mg/L (2003) and 12.6 mg/L (2017). On the other hand, during the September 2003 survey NH_4^+ showed higher contents with respect to those of NO_2^- (Nisi et al., 2005), whilst in most waters collected in October 2017, nitrite was occurring in greater amounts (Fig. 5a) with NO_2^-/NH_4^+ ratios up to 70 (i.e., T-Er). Specifically, the average NO_2^- contents were 0.60 mg/L, in September 2003, and 1.75 mg/L, in autumn 2017, while those of NH_4^+ were 1.14 and 0.37 mg/L in 2003 and 2017, respectively.

The overall contribution of nitrogenated species to the water quality (i.e., influence factor, IF_x), calculated according to eq. (1), varies from 9 % (T-El (2)) to 63 % (T-Us (3)), with an average influence of 28 %. Among them, the highest impact on water quality is ascribable to nitrite (13.5 %), especially in AR-8 and AR-9, where IF_{NO2} is > 35 %, whilst the average contribution of NO_3^- and NH_4^+ is 6.5 % and 8.1 %, respectively. Considering the values from Nisi et al. (2005), NH_4^+ has a higher IF than NO_2^- (15.8 vs. 10.1 %) and NO_3^- shows an almost equal impact (6.1 %).

In order to adopt suitable actions to implement water management, reduce nitrogenated species contents, and improve water quality, the identification of the primary sources of N-species is of paramount importance (Nisi et al., 2013, 2022; Martinelli et al., 2018; Torres-Martínez et al., 2021). Accordingly, Fig. 6 explores the possible sources and processes affecting and influencing N-species (Widory et al., 2004, 2005; Nisi et al., 2013; Divers et al., 2014; Matiatos, 2016; Sanchez et al., 2017; Ogrinc et al., 2019; Zhang et al., 2019; Torres-Martínez et al., 2020). It is worth mentioning that the fields reported in Fig. 6a-d are referred to previously published studies. Specifically, those concerning NO_3^- (Fig. 6a) are widely established and frequently used for river waters (e.g., Clark and Fritz, 1997; Kendall, 1998; Mayer et al., 2002; Xue et al., 2009; Nisi et al., 2013; Torres-Martínez et al., 2021). Contrarily, the fields depicted by $\delta^{18}O\text{-}NO_2$ and $\delta^{15}N\text{-}NO_2$ in Fig. 6d are referred to oceanic waters, since they provide oxygen deficient zones where NO_2^- can be accumulated (Casciotti, 2009, 2016). Nevertheless, they can be extended to different environments where similar conditions may occur (e.g., Lewicka-Szczebak et al., 2021).

According to Fig. 6a, the NO_3^- isotopes of the ARB waters can be referred to inputs due to soil and sewage/manure. This is also confirmed by the results obtained from the EMMTE modeling which indicates a possible average contribution deriving from soil organic nitrogen (SON) around 60 % while that of sewage and manure (SM) slightly higher than 30 % (Fig. 7a), with peak values for SM detected at T-Pe and T-Ch with an estimated contribution of 83 % and 85 %, respectively (Fig. 7b). Contrarily, T-Eg falls closer to the mineral fertilizers field with an estimated contribution deriving from chemical fertilizers (CF) around 57 %, which, on the other hand, is minimal (<5 %) in all other samples (Fig. 7a).

Moreover, the process of denitrification (i.e., reduction of NO_3^- to N_2) is apparently not affecting, or at a very minor extent, the isotopic values of the ARB waters (Appendix A Fig. S1). The limited role of denitrification seems to be also supported by the relatively small differences between the $\delta^{15}N\text{-}NO_3$ and $\delta^{15}N\text{-}NO_2$ values that are ranging from +4.7 to +15.6 ‰ (except for T-El (1), showing a difference between $\delta^{15}N\text{-}NO_3$ and $\delta^{15}N\text{-}NO_2$ equal to −2.1 ‰). Such values are lower than those commonly affecting denitrification processes (+30 ‰ ~ +50 ‰) that would further enrich $\delta^{15}N\text{-}NO_3$ with respect to $\delta^{15}N\text{-}NO_2$ (Aharoni et al., 2022). This bacterially mediated reaction is generally favored in reducing conditions (with low O_2) (Kendall, 1998), whereas oxidizing conditions prevail in the ARB.

The data from Nisi et al. (2005), representing the first and only results ever published for $\delta^{15}N\text{-}NO_3$ and $\delta^{18}O\text{-}NO_3$ in the ARB, substantially agree with those presented in this study. In fact, the water samples fall in the same fields, or close (sewage and manure) to those of the present study, except for AR-1 which is included within the mineral fertilizers field (Fig. 6a), though its isotopic ratios were not determined during the 2017 survey due to the low contents of nitrate and nitrite (Table 3). It is worth highlighting that the oxygen and nitrogen iso-

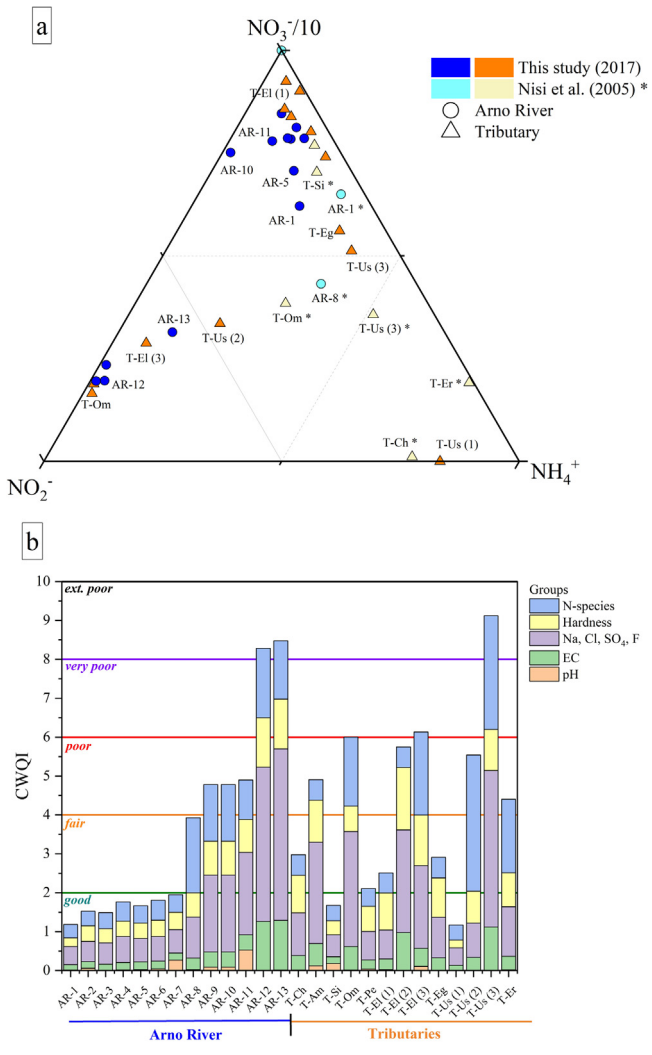

Fig. 5 – (a) NO_2^--NO_3^-/10-NH_4^+ ternary diagram for the ARB waters from this study and from Nisi et al. (2005). (b) Specific contributions of the various parameters to the CWQI, grouped as pH, EC, hardness, N-species (NO_3^-, NO_2^-, NH_4^+) and (F^-, Cl^-, Na^+, SO_4^{2-}). The length of the bars corresponds to the CWQI and the contribution by each group is computed as the CWQI*weights (w_i), according to Chemeri et al. (2023). The CWQI ranking classes (i.e., good, fair, poor, very poor and extremely poor) are also reported. IDs as reported in Table 1.

topic values from Nisi et al. (2005) have a wider range of variation and more positive values when compared to our data, which is likely a consequence of the denitrification processes that appear negligible during the 2017 survey. This evidence may indicate a slight change in the redox status during the two surveys, with more oxidizing conditions in Autumn 2017 with respect to September 2003. This would also explain the different abundances of NO_2^- and NH_4^+, as highlighted in Fig. 5a. The predominant role of nitrification during the 2017 survey is also consistent with the high NO_2^-/NH_4^+ ratios, suggesting favorable conditions for rapid NH_4^+ consumption. Moreover, a slight lowering of both δ^{15}N-NO_3 and δ^{15}N-NO_2 values was detected for these waters showing high NO_2^- (> 1 mg/L) (i.e., AR-8, AR-9, T-Er, T-Om) providing a further support to the occurrence of nitrification (Appendix A Fig. S4).

To better constrain the possible primary sources of NO_3^-, its contents are compared to those of Na^+ and Cl^-, for which a contribution by anthropogenic inputs in the ARB was established (Cortecci et al., 2002; Nisi et al., 2005, 2008a). In Fig. 6b, the NO_3/Na vs. Cl/Na (as molar ratios) diagram is reported. Based on the chemical ratios between these solutes, it is possible to identify two main components: i) the "communal effluent", characterized by NO_3/Na molar ratios around 0.05–0.15 and Cl/Na ratios between 0.5 and 1, the latter being related to domestic wastewaters (= sewage), and ii) the "agricultural component", showing higher NO_3/Na ratios approaching 10 and Cl/Na ratio between 3 and 5, usually implying the use of fertilizers (e.g., Roy et al., 1999; Nisi et al., 2013). The ARB waters are distributed close to and inside the communal effluent field (together with those from Nisi et al., 2005), apart from T-Us (2) which showed an enrichment in Cl^- with respect to Na^+, whilst AR-12 and AR-13 tend to be shifted toward the seawater field. The presence of NO_3^- contributions deriving from sewage and domestic waste is also confirmed by Fig. 6c, where the NO_3/Cl molar ratios are compared to the Cl^- contents (in μmol/L). Most waters fall within the sewage field with some diversion related to high contents in chloride. However, AR-1, AR-2, and AR-3, collected in the upper reaches of the Arno River and before the confluence with the first main tributary (T-Ch), are included in the soil "organic nitrogen" field suggesting a geogenic source of nitrate (e.g., released or leached from organic matter trapped in soil or sediments) (Fig. 7a, b). Additionally, those samples (AR-1 to AR-3) meandering in areas where the anthropogenic impact is relatively low show a good quality status (CWQI < 1.51). It is worth noticing that the nitrogen and oxygen isotopes of AR-2 and AR-3 do not fall within the soil field (Fig. 6a), confirming that the sole use of isotopic ratios, if not coupled with major ions, may lead to inconclusive or misleading results, since the extreme variability of natural systems produce overlapping ranges for the different sources as already highlighted by many authors (e.g., Nisi et al., 2013; Minet et al., 2017; Zhu et al., 2019, Torres-Martínez et al., 2021; Guo et al., 2020).

The δ^{18}O-NO_2 and δ^{15}N-NO_2 values are plotted in Fig. 6d and compared to the possible NO_2^- sources and the main processes affecting nitrite in aqueous solution (Casciotti, 2009, 2016; Buchwald and Casciotti, 2010). Most water samples (i.e., AR-8, AR-9, AR-10, AR-11, AR-12, AR-13, T-Er, T-El (3), T-Om, T-Us (2), T-Us (3)) tend to be positioned between the ammonia oxidation field and nitrite oxidation trend, indicating that the process of nitrification is affecting the ARB waters and controlling the occurrence and abundance of the reduced nitrogenated species. The nitrification process is particularly evident for those samples characterized by high contents of NO_2^- (Fig. 6d and Appendix A Fig. S1c, d). Therefore, the isotopic signature suggests that nitrogen is initially released into the waters as NH_4^+ (fresh pollution) that is easily oxidized to NO_2^-. Samples with low NO_2^- concentrations (i.e., AR-7, 0.05 mg/L; T-Si, 0.05 mg/L; T-Am, 0.06 mg/L; T-Eg, 0.04 mg/L) are distributed toward the abiotic equilibration indicating that microbially mediated reactions, such as nitrification or denitrification, are not favored. Thus, these reactions are not influencing (or only to a limited extent) the nitrite abundance due to (1) unfavorable physicochemical and kinetic conditions, (2) absence of bacterial communities able to trigger them, and/or (3) low NH_4^+ contents consumed to form NO_2^-. Finally, T-El (1) falls within the nitrite assimilation field, the biological process that converts inorganic nitrogen to ammonia and eventually, to organic nitrogen (Solomonson and Spehar, 1977). Contrarily to findings in other river systems (Li et al., 2019; Xie et al., 2020), seawater intrusion recognized at samples AR-12 and AR-13, does not seem able to affect the dissolved N-species at the mouth of the Arno River, being these samples characterized by consistent values of the N-bearing species (Table 2) and NO_3^- and NO_2^- isotopic ratios (Table 3), when compared to other samples. Eventually, it is important to consider that this geochemical survey was carried out in autumn 2017. This may partially limit the interpretation of geochemical and isotopic data, since seasonal dynamics (such as agricultural runoff, rainfall, and microbiological activity) can influence and alter the main processes occurring within the river basin.

5. Summary and conclusions

The geochemical investigation carried out in the Arno River Basin showed that the waters flowing upstream of Florence (Chiana,

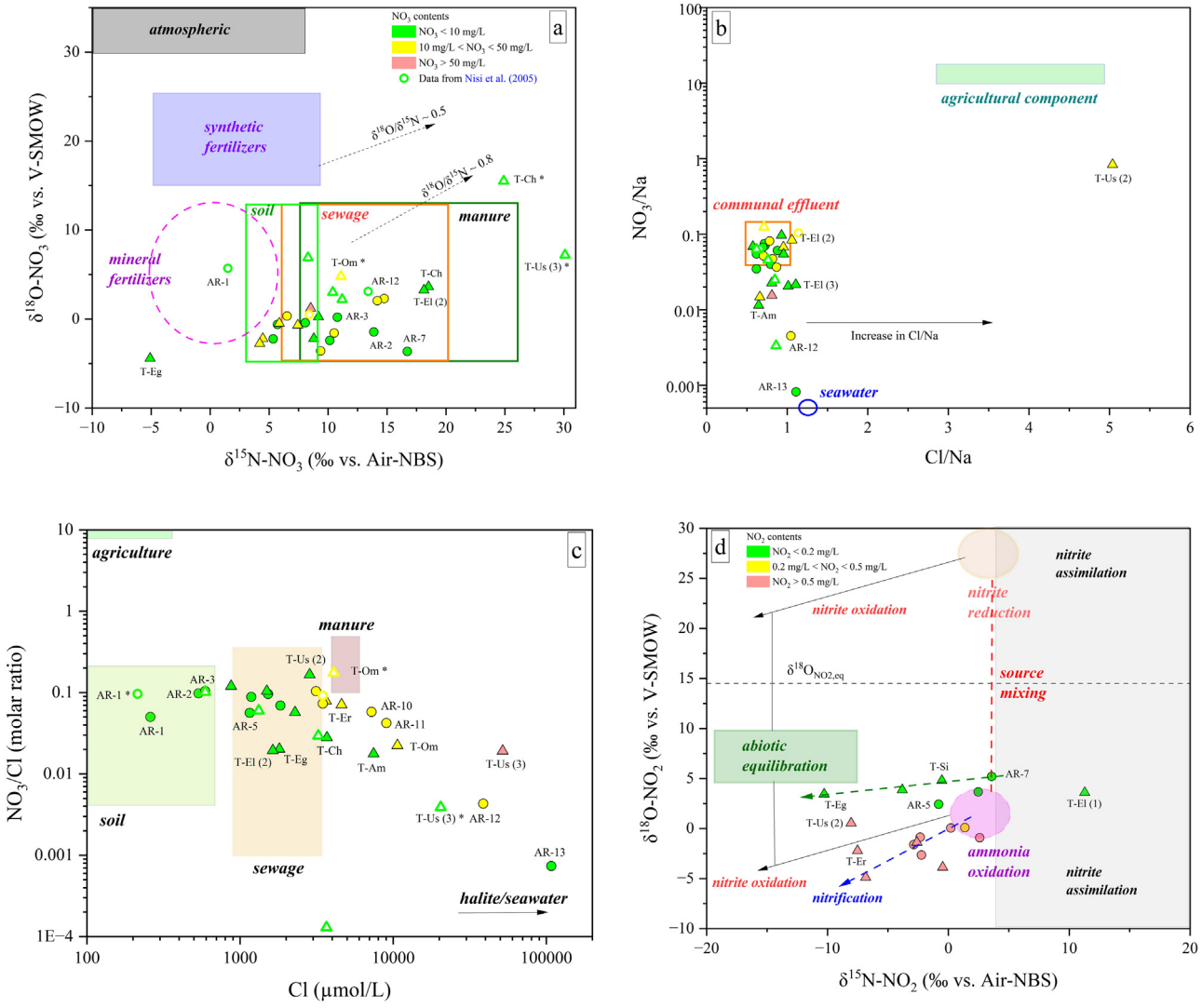

Fig. 6 – (a) Oxygen and nitrogen isotopic composition of NO_3^- for the ARB waters. The fields of the most likely NO_3^- sources are reported following Clark and Fritz (1997), Kendall (1998), Xue et al. (2009), Fenech et al. (2012), and Torres-Martínez et al. (2021). The dashed arrows describe the isotopic enrichment trends of δ^{15}N-NO_3 and δ^{18}O-NO_3 during denitrification (Mengis et al., 1999; Fukada et al., 2003); (b) NO_3/Na v. Cl/Na (as molar ratios) binary plot. Communal effluent and agricultural component fields are from Roy et al. (1999), and seawater end-member (s.w.) from Nordstrom et al. (1979); (c) NO_3/Cl (as molar ratios) vs. Cl (in μmol/L) binary plot. Fields of agricultural, soil, sewage, and manure inputs are reported following Torres-Martinez et al. (2021). (d) Oxygen and nitrogen isotopic composition of NO_2^- for ARB waters. Possible sources, sinks, and processes affecting nitrite are taken from Casciotti (2009, 2016) and Buchwald and Casciotti (2010). IDs as reported in Table 1. Symbols as reported in Fig. 1. Colors refer to NO_3^- and NO_2^- contents in the investigated samples as indicated in (a) and (d). Data from Nisi et al. (2005) are also drawn in (a), (b) and (c) (edge colored according to NO_3^- contents).

Casentino, Upper Valdarno, and Sieve sub-basins) are characterized by a relatively good quality status (CWQI < 4), with a geochemical composition mostly controlled by water-rock interactions with carbonate and silicate minerals. Contrarily, in the Middle and Lower Valdarno sub-basins, the enrichments in Na^+, Cl^-, and SO_4^{2-} lead to a notable deterioration of water quality (CWQI up to 9). These geochemical changes are related to the increasing anthropogenic burden along the ARB due to human-related pollutants supplied by tributaries, geogenic inputs by both interaction processes between surface and evaporitic rocks and discharge of thermo-mineral waters and, finally, seawater intrusion into the main course.

The Middle and Lower Valdarno sub-basins also display critical values of N-species, especially NO_2^-. The δ^{15}N and δ^{18}O isotopic data indicate that the primary sources of nitrate in the ARB waters are soil organic nitrogen (geogenic origin) and sewage and domestic wastes with minimal-to-negligible inputs from agriculture and fertilizers, as also supported by the EMMTE source apportionment modeling.

The NO_2^- isotopic data (and NO_2/NH_4 ratios) are indicative of nitrification processes that control the occurrence and relative abundance of the nitrogenated species in the ARB. Nitrite mainly derives from the oxidation of NH_4^+, the former being consequently oxidized to produce NO_3^-, which is the most abundant and stable N-bearing species in surface waters. However, a limited influence of denitrification processes for those waters showing low NO_3^- and NO_2^- contents cannot be ruled out. It is also worth noticing that currently only few δ^{15}N- and δ^{18}O-NO_2 data are available in the literature for surface waters and, consequently, this paper represents an important contribution for better understanding the chemical-isotopic processes occurring in the aquatic environment and involving NO_2^-.

The present study demonstrates that the δ^{15}N and δ^{18}O pairs in NO_3^- and NO_2^- represent a useful tool to assess and trace the geochemical processes affecting the N-species, especially when these data are combined with a detailed chemical analysis. Our results indicate that the ARB waters have had little progress in terms of environmental improvement

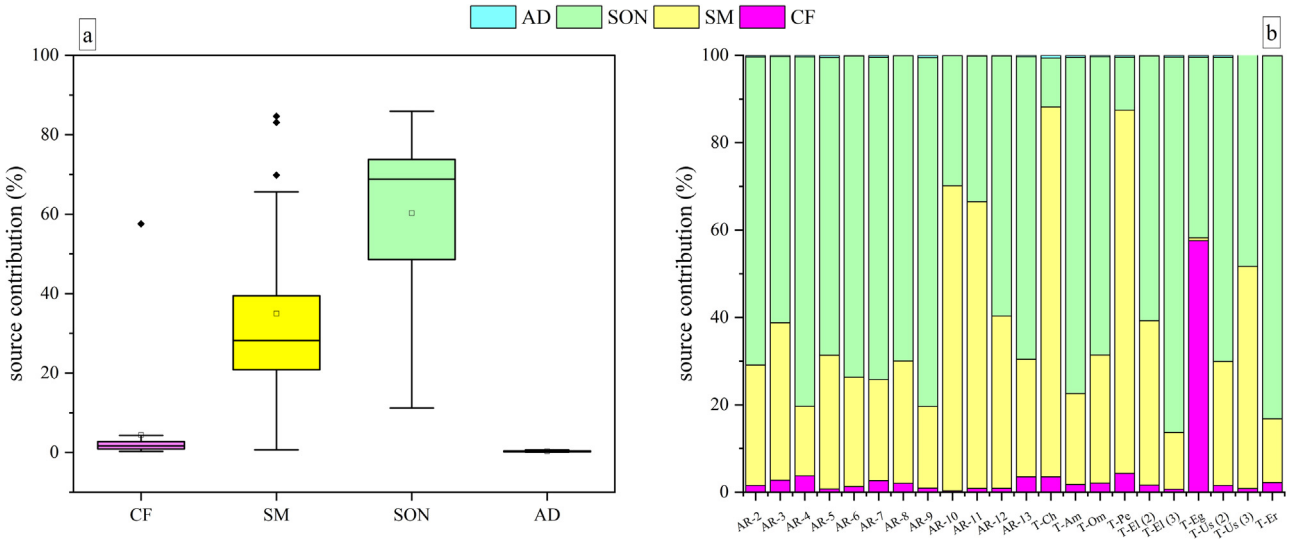

Fig. 7 – (a) Proportional (average) contributions of the main potential NO_3^- sources estimated by the EMMTE approach proposed by Cao et al. (2023). The box plots illustrate the 25th, 50th, and 75th percentiles; (b) estimated proportional contributions for each sample. The different sources are reported in different colors according to the legend: chemical fertilizers (CF, purple), atmospheric deposition (AD, light blue), soil organic nitrogen (SON, green) and manure and sewage (MS, yellow). IDs as reported in Table 1.

when compared to the investigations carried out in the early 2000s. Finally, it can be suggested that the geochemical and isotopic approach adopted in this study can be useful to design remediation or prevention actions to improve the water management and quality in the Arno River and other basins affected by notable anthropic pressure.

Declaration of competing interest

The authors declare that they have no known competing financial interests or personal relationships that could have appeared to influence the work reported in this paper.

CRediT authorship contribution statement

Lorenzo Chemeri: Writing – review & editing, Writing – original draft, Visualization, Validation, Investigation, Data curation, Conceptualization. **Barbara Nisi:** Writing – review & editing, Supervision, Methodology, Investigation, Formal analysis, Conceptualization. **Andrea Pierozzi:** Methodology, Investigation, Formal analysis, Data curation, Conceptualization. **Jacopo Cabassi:** Writing – review & editing, Investigation. **Marco Taussi:** Writing – review & editing, Visualization, Investigation. **Stefania Venturi:** Writing – review & editing, Validation, Investigation. **Antonio Delgado Huertas:** Writing – review & editing, Validation, Resources, Methodology, Investigation, Formal analysis. **Orlando Vaselli:** Writing – review & editing, Supervision, Resources, Methodology, Investigation, Formal analysis, Conceptualization.

Acknowledgments

The authors thank Dr. A. Granados, Dr. R. Campanero and Dr. S. Valiente (IACT. CSIC-UGR, Granada, Spain) for the support provided during the isotopic analysis. Prof. M. Vetuschi Zuccolini and Dr. R. Biagi are warmly thanked for the hints and support provided during date treatment and modeling elaborations. The editor and three anonymous reviewers are also thanked for their comments and suggestions that helped to improve our work.

Appendix A Supplementary data

Supplementary material associated with this article can be found in the online version at doi:10.1016/j.jes.2025.03.064.

References

Abascal, E., Gomez-Coma, L., Ortiz, I., Ortiz, A., 2022. Global diagnosis of nitrate pollution in groundwater and review of removal technologies. Sci. Total Environ. 810, 152233.
Abbate, R., Castellucci, P., Ferrini, G.L., Pandeli, E., 1992. I dintorni di Firenze. Guide Geol. Reg. 4, 214–223.
Aharoni, J., Dahan, O., Siebner, H., 2022. Continuous monitoring of dissolved inorganic nitrogen (DIN) transformations along the waste-vadose zone-groundwater path of an uncontrolled landfill, using multiple N-species isotopic analysis. Water Res. 219, 118508.
Andersson, K.K., Hooper, A.B., 1983. O_2 and H_2O are each the source of one O in NO_2^- produced from NH_3 by Nitrosomonas: ^{13}N-NMR evidence. FEBS Lett. 164, 236–240.
Atekwana, E.A., Krishnamurthy, R.V., 1998. Seasonal variations of dissolved inorganic carbon and $\delta^{13}C$ of surface waters: application of a modified gas evolution technique. J. Hydrol. 205, 265–278.
Baldacci, F., Elter, P., Giannini, E., Giglia, G., Lazzarotto, A., Nardi, R., et al., 1967. Nuove osservazioni sul problema della Falda Toscana e della sua interpretazione dei flysch arenacei tipo Macigno dell'Appennino Settentrionale. Mem. Soc. Geol. It. 6, 213–244.
Barth, J.A.C., Cronin, A.A., Dunlop, J., Kalin, R.M., 2003. Influence of carbonates on the riverine carbon cycle in an anthropogenically dominated catchment basin: evidence from major elements and stable carbon isotopes in the Lagan River (N. Ireland). Appl. Geoch. 200 (3–4), 203–216.
Bencini, A., Malesani, P., 1993. Fiume Arno: acque, Sedimenti e Biosfera. Accademia Toscana di Scienze e Lettere La Colombaria, Olschki S Leo Ed., Florence, Italy.
Blaisdell, J., Turyk, M.E., Almberg, K.S., Jones, R.M., Stayner, L.T., 2019. Prenatal exposure to nitrate in drinking water and the risk of congenital anomalies. Environ. Res. 176, 108553.
Bottrell, S., Hipkins, E.V., Lane, J.M., Zegos, R.A., Banks, D., Frengstad, B.S., 2019. Carbon-13 in groundwater from English and Norwegian crystalline rock aquifers: a tool for deducing the origin of alkalinity? Sustain. Water Resour. Manage. 5, 267–287.
Buchwald, C., Casciotti, K.L., 2010. Oxygen isotope fractionation and exchange during bacterial nitrite oxidation. Limnol. Oceanogr. 55 (3), 1064–1074.
Buchwald, C., Casciotti, K.L., 2013. Isotopic ratios of nitrite as tracers of the sources and age of oceanic nitrite. Nat. Geosci. 6, 308–313.
Cao, X., He, W., He, W., Shi, Y., An, T., Wang, X., et al., 2023. *EMMTE*: An Excel VBA tool for source apportionment of nitrate based on the stable isotope mixing model. Sci. Total Environ. 868, 121728.
Capri, E., Civita, M., Corniello, A., Cusimano, G., De Maio, M., Ducci, D., et al., 2009. Assessment of nitrate contamination risk: The Italian experience. J. Geochm. Expl. 102, 71–86.
Carmignani, L., Kligfield, R., 1990. Crustal extension in Northern Apennines: the transition from compression to extension in the Alpi Apuane core complex. Tectonics 9, 1275–1303.
Casciotti, K.L., 2009. Inverse kinetic isotope fractionation during bacterial nitrite oxidation. Geochim. Cosmochim. Acta 73 (7), 2061–2076.
Casciotti, K.L., 2016. Nitrite isotopes sas tracers of marine N cycle processes. Phil. Trans. R. Soc. A. 374, 20150295.
Chemeri, L., Cabassi, J., Taussi, M., Venturi, S., 2023. Development and testing of a new flexible, easily and widely applicable chemical water quality index (CWQI). J. Environ. Manage. 348, 119383.

Chemeri, L., Taussi, M., Cabassi, J., Capecchiacci, F., Randazzo, A., Tassi, F., et al., 2024. Groundwater and dissolved gases geochemistry in the Pesaro-Urbino province (northern Marche, Central Italy) as tool for seismic surveillance and sustainability. Sustainability 16 (12), 5178.

Chiodini, G., Frondini, F., Cardellini, C., Parello, F., Peruzzi, L., 2000. Rate of diffuse carbon dioxide degassing estimated from carbon balance of regional aquifers: The case of central Apennines, Italy. J. Geophys. Res. 105, 8423–8434.

Choi, W.J., Han, G.H., Lee, S.M., Lee, G.T., Yoon, K.S., Ro, H.M., 2007. Impact of land-use types on nitrate concentration and $\delta^{15}N$ in unconfined ground water in rural areas of Korea. Agric. Ecosyst. Environ. 120, 259–268.

Clark, J., Fritz, P. (Eds.), 1997. Environmental Isotopes in Hydrogeology. Lewis Publisher, Boca Raton.

Cortecci, G., Boschetti, T., Dinelli, E., Cidu, R., Podda, F., Doveri, M., 2009. Geochemistry of trace elements in surface waters of the Arno River Basin, northern Tuscany, Italy. Appl. Geochem. 24 (5), 1005–1022.

Cortecci, G., Dinelli, E., Boschetti, T., 2007. The River Arno catchment, northern Tuscany: chemistry of waters and sediments from the River Elsa and River Era sub-basins, and sulphur and oxygen isotopes of aqueous sulphate. Hydrol. Process. 21 (1), 1–20.

Cortecci, G., Dinelli, E., Bencini, A., Adorni Braccesi, A., La Ruffa, G., 2002. Natural and anthropogenic SO_4 sources in the Arno River catchment, Northern Tuscany, Italy: a chemical and isotopic reconnaissance. Appl. Geochem. 17 (2), 79–92.

Conti, P., Cornamusini, G., Carmignani, L., 2020. An outline of the geology of the Northern Apennines (Italy), with geological map 1:250.000 scale. Ital. J. Geosci. 139 (2), 149–194.

Denk, T.R.A., Mohn, J., Decock, C., Lewika-Szczebak, D., Harris, E., Butterbach-Bahl, K., et al., 2017. The nitrogen cycle: A review of isotope effects and isotope modelling approaches. Soil Biol. Biochem. 105, 121–137.

D'Oria, M., Ferraresi, M., Tanda, M.G., 2019. Quantifying the impacts of climate change on water resources in northern Tuscany, Italy, using high resolution regional projections. Hydrol. Process. 33 (6), 889–1028.

Di Matteo, L., Dragoni, W., Maccari, D., Piacentini, S.M., 2017. Climate change, water supply and environmental problems of headwaters: the paradigmatic case of the Tiber, Savio and Marecchia rivers (Central Italy). Sci. Total Environ. 598, 733–748.

Dinelli, E., Cortecci, G., Lucchini, F., Zantedeschi, E., 2005. Sources of major and trace elements in the stream sediments of the Arno River catchment (northern Tuscany, Italy). Geochem. J. 39 (6), 531–545.

Divers, M.T., Elliott, E.M., Bain, D.J., 2014. Quantification of nitrate sources to an urban stream using dual nitrate isotopes. Environ. Sci. Technol. 48 (18), 10580–10587.

Egidio, E., Mancini, S., De Luca, D.A., Lasagna, M., 2022. The impact of climate change on groundwater temperature of the Piedmont Po Plain (NW Italy). Water (Basel) 14, 2797.

EU Directive 1991/676/ECC, 1991. Council Directive of 12 December 1991 concerning the protection of water against the pollution caused by nitrates from agricultural sources. Off. J. Euro. Union 2.12.1991.

EU Directive 2000/60/EC, 2000. Council Directive of 23 October 2000 establishing a framework for Community action in the field of water policy. Off. J. Euro Union 23.10.2000.

EU Directive 2020/2184/EC, 2020. Council Directive of 16 December 2020 on the quality of water intended for human consumption. Off. J. Euro. Union L 435 23.12.2020.

Fenech, C., Rock, L., Nolan, K., Tobin, J., Morrisey, A., 2012. The potential for a suite of isotope and chemical markers to differentiate sources of nitrate contamination: A review. Water Res. 46 (7), 2023–2041.

Fukada, T., Hiscock, K.M., Dennis, J.P., Grischeck, T., 2003. A dual isotope approach to identify denitrification in ground water at a river bank infiltration site. Water Res. 37 (13), 3070–3078.

Gaillardet, J., Dupré, B., Allègre, C.J., Négrel, P., 1997. Chemical and physical denudation in the Amazon River Basin. Chem. Geol. 142 (3-4), 141–173.

Galloway, J.N., Townsend, A.R., Erisman, J.W., Bekunda, M., Cai, Z., Freney, J.R., et al., 2008. Transformation of the nitrogen cycle: recent trends, questions, and potential solutions. Science 320 (8578) 889–892.

Giani, P., Panichi, C., 2003. Caratterizzazione chimico-isotopica del Fiume Arno nel tratto terminale con particolare riferimento all'interazione con gli acquiferi nella piana di Pisa. S. T. A. R. Servizio Tecnografico Area della Ricerca del CNR, pp. 94.

Grassa, F., Capasso, G., Favara, R., Inguaggiato, S., 2006. Chemical and isotopic composition of waters and dissolved gases in some thermal springs of Sicily and adjacent Volcanic Island, Italy. Pure Appl. Geophys. 163 (4), 781–807.

Grimmeisen, F., Lehmann, M.F., Liesch, T., Goeppert, N., Klinger, J., Zopfi, J., et al., 2017. Isotopic constrains on water source mixing, network leakage and contamination in an urban groundwater system. Sci. Total Environ. 583, 202–213.

Guo, Z., Yan, C., Wang, Z., Xu, F., Yang, F., 2020. Quantitative identification of nitrate sources in a coastal peri-urban watershed using hydrogeochemical indicators and dual isotopes together with the statistical approaches. Chemosphere 243, 125364.

Gupta, P., Singh, J., Verma, S., Chandel, A.S., Bhatla, R., 2021. Chapter 1 – impact of climate change and water quality degradation on food security and agriculture. In: Thokchom, B., Qiu, P.P., Singh, P., Iyer, P.K. (Eds.), Water Conservation in the Era of Global Climate Change. Elsevier, pp. 1–22.

Kachroud, M., Trolard, F., Kefi, M., Jebari, S., Bourrié, G., 2019. Water quality indices: challenges and application limits in the literature. Water (Basel) 11 (2), 361.

Kendall, C., 1998. Tracing nitrogen sources and cycling in catchments. In: Kendall, C., McDonnell, J.J. (Eds.), Isotope-tracers in Catchment Hydrology. Elsevier, Amsterdam, pp. 519–576.

Kharbush, J.J., Robinson, R.S., Carter, S.J., 2023. Patterns in sources and forms of nitrogen in a large eutrophic scale during a cyanobacterial harmful algae bloom. Limnol. Oceanogr. 68 (4), 803-815.

Lewika-Szczebak, D., Jansen-Willems, A., Muller, C., Dyckmans, J., Well, R., 2021. Nitrite isotope characteristics and associated N soil transformation. Sci. Rep. 11, 5008.

Li, X., Tang, C., Cao, Y., Li, X., 2019. Carbon, nitrogen and sulfur isotopic features and the associated geochemical processes in a coastal aquifer system of the Pearl River Delta, China. J. Hydrol. 579, 986–998.

Linhoff, B., 2022. Deciphering natural and anthropogenic nitrate and recharge sources in arid region groundwaters. Sci. Total Environ. 848, 157345.

Martinelli, G., Dadomo, A., De Luca, D.A., Mazzola, M., Lasagna, M., Pennisi, M., et al., 2018. Nitrate sources, accumulation and reduction in groundwater from Northern Italy: insights provided by a nitrate and boron isotopic database. Appl. Geochem. 91, 23–35.

Martinez-Navarrete, C., Grima Olmedo, J., Duran Valsero, J.J., Gomez, J.D., Luque Espinar, J.A., de la Orden, G.J.A., 2008. Groundwater protection in Mediterranean countries after the European water framework directive. Environ. Geol. 54, 537–549.

Matiatos, I., 2016. Nitrate source identification in groundwater of multiple land-use areas by combining isotopes and multivariate statistical analysis: a case study of Asopos basin (Central Greece). Sci. Total Environ. 514, 802–814.

Matiatos, I., Moeck, C., Vystavna, Y., Marttila, H., Orlowski, N., Jessen, S., et al., 2023. Nitrate isotopes in catchment hydrology: Insights, ideas and implications for models. J. Hydrol. 626, 130326.

Matiatos, I., Wassenaar, L.I., Monteiro, L.R., Venkiteswaran, J.J., Goody, D.C., Boeckx, P., et al., 2021. Global patterns of nitrate isotope composition in rivers and adjacent aquifers reveal reactive nitrogen cascading. Commun. Earth. Environ. 2 (1), 1–10.

Mayer, B., Boyer, E.W., Goodale, C., Jaworski, N.A., Breemen, N.V., Howarth, R.W., et al., 2002. Sources of nitrate in rivers draining watersheds in the northeastern US: isotopic constraints. Biogeochemistry 57 (1), 171–197.

McIlvin, M.R., Altabet, M.A., 2005. Chemical conversion of nitrate and nitrite to nitrous oxide for nitrogen and oxygen isotopic analysis in freshwater and seawater. Anal. Chem. 77 (17), 5589–5595.

Mengis, M., Schiff, S.L., Harris, M., English, M.C., Aravena, R., Elgood, R.J., et al., 1999. Multiple geochemical and isotopic approaches for assessing ground water NO_3^- elimination in a riparian zone. Ground Water 37 (8), 448–457.

Miller, J.D., Hutchins, M., 2017. The impacts of urbanization and climate change on urban flooding and urban water quality: A review of the evidence concerning the United Kingdom. J. Hydrol: Region. Stud. 12, 345–362.

Minet, E.P., Goodhue, R., Meier-Augenstein, W., Kalin, R.M., Fenton, O., Richards, K.G., et al., 2017. Combining stable isotopes with contamination indicators: A method for improved investigation of nitrate sources and dynamics in aquifers with mixed nitrogen inputs. Water Res. 124, 85-96.

Minissale, A., 2004. Origin, transport and discharge of CO_2 in central Italy. Earth Sci. Rev. 66 (1), 89–141.

Nisi, B., Buccianti, A., Vaselli, O., Perini, G., Tassi, F., Minissale, A., et al., 2008a. Hydrogeochemistry and strontium isotopes in the Arno River Basin (Tuscany, Italy): constraints on natural controls by statistical models. J. Hydrol. 360 (1-4), 166–183.

Nisi, B., Vaselli, O., Buccianti, A., Minissale, A., Delgado Huertas, A., Tassi, F., et al., 2008b. Indagine geochimica ed isotopica del carico disciolto nelle acque di scorrimento superficiale della valle dell'Arno: valutazione del contributo naturale ed antropico. Mem. Descr. Carta Geol. d'It. pp.160.

Nisi, B., Vaselli, O., Buccianti, A., Silva, S.R., 2005. Sources of nitrate in the Arno River waters: constraints $\delta^{15}N$ and $\delta^{18}O$. GeoActa 4, 13–24.

Nisi, B., Vaselli, O., Delgado Huertas, A., Tassi, F., 2013. Dissolved nitrates in the groundwater of the Cecina Plain (Tuscany, Central-Western Italy): clues from the isotopic signature of NO_3^-. Appl. Geochem. 34, 38–52.

Nisi, B., Vaselli, O., Taussi, M., Doveri, M., Menichini, M., Cabassi, J., et al., 2022. Hydrogeochemical surveys of shallow coastal aquifers: a conceptual model to set-up a monitoring network and increase the resilience of a strategic groundwater system to climate change and anthropogenic pressure. Appl. Geochem. 142, 105350.

Nordstrom, D.K., Plummer, L.N., Wigley, T.M.L., Wolery, T.J., Ball, J.W., Jenne, E.A., et al., 1979. Chemical modeling in aqueous systems. Am. Chem. Soc. Symp. Ser. 93, 857–892.

Ogrinc, N., Tamse, S., Zavadlav, S., Vrzel, J., Jin, L., 2019. Evaluation of geochemical processes and nitrate pollution sources at the Ljubljansko polje aquifer (Slovenia): a stable isotope perspective. Sci. Total Environ. 646, 1588e1600.

Raco, B., Vivaldo, G., Doveri, M., Menichini, M., Masetti, G., Battaglini, R., et al., 2021. Geochemical, geostatistical, and time series analysis techniques as a tool to achieve the Water Framework Directive goals: an example from Piedmont region (NW Italy). J. Geochem. Expl. 229, 106832.

Regione Toscana, 2019. DB UCS 1:10000 (database of land use and soil cover).

Roy, S., Gaillardet, J., Allègre, C.J., 1999. Geochemistry of dissolved and suspended loads of the Seine River, France. Anthropogenic impact, carbonate and silicate weathering. Geochim. Cosmochim. Acta 63, 1277–1292.

Salata, G.G., Roelke, L.A., Cifuentes, L.A., 2000. A rapid and precise method for measuring stable isotope ratios of dissolved inorganic carbon. Mar. Chem. 69, 153–161.

Salerno, F., Gaetano, V., Tartari, G., 2018. Urbanization and climate change impacts on surface water quality: enhancing the resilience by reducing impervious effects. Water Res. 144, 491–502.

Sanchez, D.A., Szynkiewicz, A., Faiia, A.M., 2017. Determining sources of nitrate in the semi-arid Rio Grande using nitrogen and oxygen isotopes. Appl. Geochem. 86, 59–69.

Schindler, D.W., 2006. Recent advances in the understanding and management of eutrophication. Limnol. Oceanogr. 51 (1), 356–363.

Schullehner, J., Hansen, B., Thygesen, M., Pedersen, C.B., Sigsgaard, T., 2018. Nitrate in drinking water and colorectal cancer risk: a nationwide population-based cohort study. Int. J. Cancer 143, 73–79.

Shi, H., Du, Y., Xiong, Y., Deng, Y., Li, Q., 2024. Source-oriented health risk assessment of groundwater nitrate by using EMMTE coupled with HHRA model. Sci. Total Environ. 934, 173283.

Solomonson, L.P., Spehar, A.M., 1977. Model for regulation of nitrate assimilation. Nature 265, 373–375.

Taussi, M., Gozzi, C., Vaselli, O., Cabassi, J., Menichini, M., Doveri, M., et al., 2022. Contamination assessment and temporal evolution of nitrates in the shallow aquifer of the Metauro River Plain (Adriatic Sea, Italy) after remediation. J. Environ. Res. Pub. Health 19, 12231.

Taussi, M., Vespasiano, G., Chemeri, L., Bonì, R., Nisi, B., Vaselli, O., et al., 2024. Assessing anthropogenic and natural influences on water quality in a critical shallow groundwater system: insights from the Metauro River basin (Central Italy). Groundw. Sustain. Dev. 27, 101361.

Tognotti, L., Andreussi, P., Ciandri, P., Bonucelli, M., Spinetti, S., Rizzuti, E., et al., 1998. Monitoring and control of the Arno River pollution in the leather manufacturing district. Final Report of LIFE Project, EC94/IT/A25/IT00464.

Torres-Martínez, J.A., Mora, A., Knappett, P.S.K., Ornelas-Sotos, N., Mahlknecht, J., 2020. Tracking nitrate and sulfate sources in groundwater of an urbanized valley using a multi-tracer approach combined with a Bayesian isotope mixing model. Water Res. 182, 115962.

Torres-Martínez, J.A., Mora, A., Mahlknecht, J., Daesslé, L.W., Cervantes-Avilés, P.A., Ledesma-Ruiz, R., 2021. Estimation of nitrate pollution sources and transformations in groundwater of an intense livestock-agricultural area (Comarca, Lagunera), combining major ions, stable isotopes and MixSTAR model. Enviro. Pollut. 269, 115445.

Uddin, M.G., Nash, S., Olbert, A.G., 2021. A review of water quality index models and their use for assessing surface water quality. Ecol. Indic. 122, 107218.

Ward, M.H., Jones, R.R., Brender, J.D., De Kok, T.M., Weyer, P.J., Nolan, B.T., et al., 2018. Drinking water nitrate and human health: an updated review. Int. J. Environ. Res. Pub. Health 15, 1557.

Wells, N.S., Hakoun, V., Brouvère, S., Knoller, K., 2016. Multi-species measurements of nitrogen isotopic composition reveal the spatial constrains and biological drivers of ammonium attenuation across a highly contaminated groundwater system. Water Res. 98, 363–375.

Widory, D., Kloppmann, W., Chery, L., Bonnin, J., Rochdi, H., Guinamant, J.L., 2004. Nitrate in groundwater: an isotopic multi-tracer approach. J. Contam. Hydrol. 72, 165–188.

Widory, D., Petelet-Giraud, E., Négrel, P., Ladouche, B., 2005. Tracking the source of nitrate in groundwater using coupled nitrogen and boron isotopes: a synthesis. Environ. Sci. Technol. 39, 539–548.

Xie, R., Rao, P., Pang, Y., Shi, C., Li, J., Shen, D., 2020. Salt intrusion alters nitrogen cycling in tidal reaches as determined in field and laboratory investigations. Sci. Total Environ. 729, 138803.

Xue, D., Botte, J., Baets, B.D., Accoe, F., Nestler, A., Taylor, P., et al., 2009. Present limitations and future prospects of stable isotope methods for nitrate source identification in surface- and groundwaters. Water Res. 43, 1159–1170.

Zhang, Y., Shi, P., Song, J., Li, Q., 2019. Application of nitrogen and oxygen isotopes for source and fate identification of nitrate pollution in surface water: a review. Appl. Sci. 9 (1), 18.

Zhu, A., Chen, J., Gao, L., Shimizu, Y., Liang, D., Yi, M., et al., 2019. Combined microbial and isotopic signature approach to identify nitrate sources and transformation processes in groundwater. Chemosphere 228, 721-734.